University of Pennsylvania
ScholarlyCommons

Departmental Papers (ESE) Department of Electrical & Systems Engineering

6-29-2009

Integrated Aluminum Nitride Piezoelectric Microelectromechanical System for Radio Front Ends

Gianluca Piazza
University of Pennsylvania, piazza@seas.upenn.edu

Follow this and additional works at: http://repository.upenn.edu/ese_papers

Part of the Electrical and Computer Engineering Commons

Recommended Citation
Gianluca Piazza, "Integrated Aluminum Nitride Piezoelectric Microelectromechanical System for Radio Front Ends", . June 2009.

Suggested Citation:
Piazza, G. (2009). "Integrated aluminum nitride piezoelectric microelectromechanical system for radio front ends." *Journal of Vacuum Science and Technology A*. vol. 27(4). pp. 776 - 784.

© 2009 American Vacuum Society. This article may be downloaded for personal use only. Any other use requires prior permission of the author and the American Vacuum Society. The following article appeared in *Journal of Vacuum Science and Technology A* and may be found at http://dx.doi.org/10.1116/1.3077276.

This paper is posted at ScholarlyCommons. http://repository.upenn.edu/ese_papers/580
For more information, please contact repository@pobox.upenn.edu.

Integrated Aluminum Nitride Piezoelectric Microelectromechanical System for Radio Front Ends

Abstract
This article summarizes the most recent technological developments in the realization of integrated aluminum nitride (AlN) piezoelectric microelectromechanical system (MEMS) for radio frequency (rf) front ends to be employed in next generation wireless communication devices. The AlN-based resonator and switch technologies are presented, their principle of operation explained, and some key experimental achievements showing device operations between 20 MHz and 10 GHz are introduced. Fundamental material, device, and fabrication aspects that needed to be taken into account for the demonstration of the first integrated rf MEMS solution based on the combination of AlN MEMS resonators and switches are highlighted. Given the ability to operate over a broad range of frequencies on a single silicon chip, the AlN MEMS technology is extremely attractive for the demonstration of reconfigurable and multiband rf transceivers. Next generation rf architectures that take advantage of large scale integration of AlN MEMS resonators and switches are briefly presented.

Disciplines
Electrical and Computer Engineering | Engineering

Comments
Suggested Citation:
Piazza, G. (2009). "Integrated aluminum nitride piezoelectric microelectromechanical system for radio front ends." *Journal of Vacuum Science and Technology A*. vol. 27(4). pp. 776 - 784.

© 2009 American Vacuum Society. This article may be downloaded for personal use only. Any other use requires prior permission of the author and the American Vacuum Society. The following article appeared in *Journal of Vacuum Science and Technology A* and may be found at http://dx.doi.org/10.1116/1.3077276.

This journal article is available at ScholarlyCommons: http://repository.upenn.edu/ese_papers/580

Integrated aluminum nitride piezoelectric microelectromechanical system for radio front ends

Gianluca Piazza[a)]
Department of Electrical and Systems Engineering, University of Pennsylvania, Pennsylvania 19104

(Received 2 October 2008; accepted 5 January 2009; published 29 June 2009)

This article summarizes the most recent technological developments in the realization of integrated aluminum nitride (AlN) piezoelectric microelectromechanical system (MEMS) for radio frequency (rf) front ends to be employed in next generation wireless communication devices. The AlN-based resonator and switch technologies are presented, their principle of operation explained, and some key experimental achievements showing device operations between 20 MHz and 10 GHz are introduced. Fundamental material, device, and fabrication aspects that needed to be taken into account for the demonstration of the first integrated rf MEMS solution based on the combination of AlN MEMS resonators and switches are highlighted. Given the ability to operate over a broad range of frequencies on a single silicon chip, the AlN MEMS technology is extremely attractive for the demonstration of reconfigurable and multiband rf transceivers. Next generation rf architectures that take advantage of large scale integration of AlN MEMS resonators and switches are briefly presented. *© 2009 American Vacuum Society.* [DOI: 10.1116/1.3077276]

I. INTRODUCTION

Current radio frequency (rf) systems suffer from the inability to efficiently use the available radio spectrum and rapidly reconfigure and adapt to jamming or interferers. The primary limitation of the current rf systems and to the realization of future cognitive radios with high spectral awareness resides in the absence of reconfigurable and high quality factor (Q) micromechanical filtering and frequency setting elements. Although most of the currently available rf electronic components can all be implemented in a single complementary metal oxide semiconductor (CMOS) chip, the bottleneck to the demonstration of truly compact cognitive radios lies in the off chip and bulky mechanical components currently used for filtering. The need to reconfigure the rf front end imposes the realization of arrays of filters and oscillators or tunable components that would be impractical or take on an extremely large footprint if fabricated with state-of-the-art mechanical resonators such as surface acoustic wave (SAW) and film bulk acoustic resonator[1,2] (FBAR) or LC tunable filters and with switching technologies based on field effect transistors. Furthermore, these commercially available components cannot be monolithically integrated and therefore suffer from parasitic capacitances (and consequently increased insertion loss and switching speeds) originated by the inevitable interconnects required to route the signal through different technologies. Massive arraying of AlN microelectromechanical resonators and switches on the same silicon chip can solve this fundamental bottleneck. Monolithic cofabrication of AlN microelectromechanical system (MEMS) resonators, filters, and switches will enable highly reconfigurable, spectral aware front ends. By doing so, parasitic components will be dramatically reduced and single-chip, compact, and reconfigurable transceivers delivered. Figure 1 schematically renders the front-end evolution from a single-band solution to a multiband, single-chip reconfigurable receiver that will be enabled by the monolithic integration of AlN contour-mode MEMS resonators and switches described herein.

In this article the fundamental technological developments for the realization of this single-chip AlN platform are presented from a material, device, and system perspective. AlN has been selected for its superior rf, mechanical, and piezoelectric properties. It has been proven to have high sound velocity (10 km/s), high resistivity (10^{13} Ω m), and good piezoelectric coupling coefficient, which has also made it the material of choice for a commercially successful rf resonator product such as the FBAR. The use of piezoelectric transduction renders the fabricated resonators easily interfaced with current 50 Ω rf systems (differently from what occurs in high impedance pure silicon-based technologies that use electrostatic transduction[3–5]) and can provide MEMS switches with large forces and increased reliability. The ease of manufacturing AlN devices and integrating them with CMOS electronics[6,7] make AlN the preferred material for the demonstration of fully integrated, small form-factor rf solutions.[8,9] The next sections will describe the realization and experimental demonstration of MEMS AlN resonators, filters, oscillators, and switches and highlight the key innovations that are made possible by this integrated solution.

II. MEMS ALN CONTOUR-MODE RESONATOR TECHNOLOGY

A. MEMS AlN contour-mode resonators

Contour mode of vibrations can be excited in the c-axis oriented aluminum nitride films via the d_{31} piezoelectric coefficient. By applying an electric field across the film sandwiched between a top and bottom electrode, the MEMS

a)Electronic mail: piazza@seas.upenn.edu

 0734-2101/2009/27(4)/776/9/$25.00 ©2009 American Vacuum Society

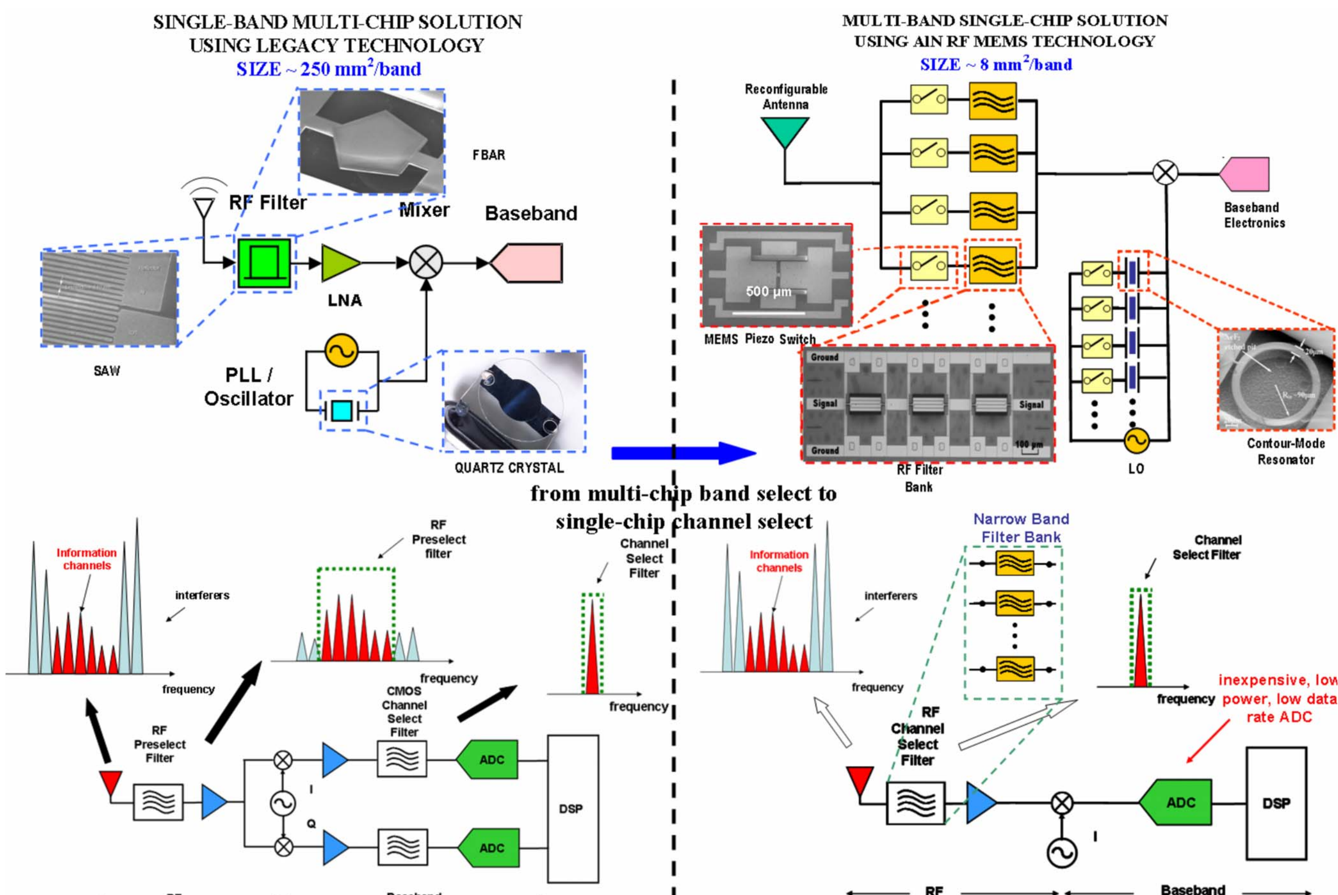

FIG. 1. (Color online) Envisioned change in rf front-end architecture made possible by the AlN rf MEMS technology. The AlN devices can substitute the existing single-band multichip solution with a multiband (or channel) single-chip implementation. Beyond that also a channel select, instead of a band select rf processing strategy can be realized with the switched narrow-band AlN filter technology. Direct sampling of incoming rf signal will enable next generation software defined radios.

structure expands laterally and can be excited in resonant vibrations whose frequency is set by one of the in-plane dimensions of the device.

The most promising structures demonstrated to obtain high Q (1000–4000) and high frequency of operations (10 MHz–1.6 GHz) are rings and rectangular plates, as shown in Table I. The frequency of vibration, f_o, is generally set by the width of the structure, W (Table I), whereas the second dimension can be employed to control the equivalent motional resistance, R_M, and static capacitance, C_o, of the device as shown in Eq. (1),

$$f_o = \frac{1}{2W} c_{\mathrm{AlN}}, \quad R_M \propto \frac{T}{nL}, \quad C_o \propto \frac{nWL}{T}, \tag{1}$$

where c_{AlN} is the sound velocity of AlN, T is the film thickness, n is the number of electrodes patterned on the AlN plate, and L is the actual length of the plate.

Either fundamental or higher order mode can be selectively excited in rectangular or annular plates (Table I) by properly patterning the top electrode and therefore defining the effective width of the resonant element. The use of higher order modes of vibration is deemed necessary in order to reduce the sensitivity to lithographic errors and misalignments for devices operating at frequencies above 400 MHz, for which the definition of small features would otherwise significantly complicate the ability to accurately set frequency. The multielectrode configuration (used to excite higher order modes) reduces the sensitivity to lithographic tolerances by relying on the definition of a precise pitch rather than an absolute dimension, as in the case of the fundamental mode device. In addition, the frequency defining element becomes the electrode (rather than the AlN films), which is thin (100–200 nm) and easier to pattern into very small features. A fundamental advantage of this resonator technology over FBAR or SAW resonators is that the device center frequency can be set exclusively at the computer aided design layout level, therefore enabling multiple frequencies of vibration on the same silicon chip, and greatly reducing manufacturing tolerances to film thicknesses.

The AlN plate can be excited into vibrations by two means of applying an electric field across the film thickness. The two most successful implementations to date[10] are based on thickness field excitation (TFE) and lateral field excitation (LFE) (Fig. 2). LFE results in a more robust implementation since it is less sensitive to electrode alignment, but suffers from reduced electromechanical coupling and effective de-

TABLE I. Summary of most significant AlN contour-mode resonators demonstrated to date.

Resonator Type	Scanning Electron Micrograph	Mode of Vibration	Electrical Response (Admittance Plot)	Demonstrated Key Features
Rectangular Plate [35]			f_s = 85.4 MHz Q = 2100 R_m = 125 Ω	- f = 20-100 MHz - Q = 1,000-3,000 - k_t^2=0.5-1.5 % - R_m = 50-300 Ω
Annular Plate [35]			f_s = 224 MHz Q = 2400 R_m = 56 Ω	- f = 100-400 MHz - Q = 1,000-4,000 - k_t^2=0.5-1.5 % - R_m = 50-300 Ω
Higher Order Rectangular Plate [36]		Contraction, Expansion, W	f_s = 527 MHz Q = 4200 R_m = 47 Ω	- f = 100-1200 MHz - Q = 1,000-4,000 - k_t^2=0.8-2.1 % - R_m = 20-300 Ω
Higher Order Annular Plate [37]		Contraction, Expansion, W, Line of symmetry with respect to center of annulus	f_s = 1.03 GHz Q = 820 R_m = 60 Ω	- f = 400-1600 MHz - Q = 500-1,200 - k_t^2=0.5-2 % - R_m = 20-300 Ω

[a]Reference 35.
[b]Reference 36.
[c]Reference 37.

vice reactance, which simultaneously make the resonator interface with external circuitry more complicated. For these reasons, TFE is the preferred embodiment, although LFE can still be employed where it is advantageous to do so. Experimental results extracted for resonators operating at 85, 224, 527 MHz, and 1.03 GHz are shown in Table I. These devices show relatively low motional impedances (ranging from 50 to 300 Ω), Qs in air varying from 800 (at the highest frequency) to 4200, and electromechanical coupling coefficients, k_t^2, ranging from 0.5% to 2.1%. The device fQ product has reached a value of 4.6×10^{12}, and has counterintuitively been increasing with frequency (Fig. 3). These data show the promise of this technology that has been employed to demonstrate working prototypes of oscillators and filters, but also highlight how further improvements are possible in terms of Q factor enhancement. In fact, historically, most resonant devices have shown to follow a constant fQ curve.[11] Therefore it should be possible to attain even higher Qs at the frequencies of more direct interest for rf communications (10 MHz–3 GHz).

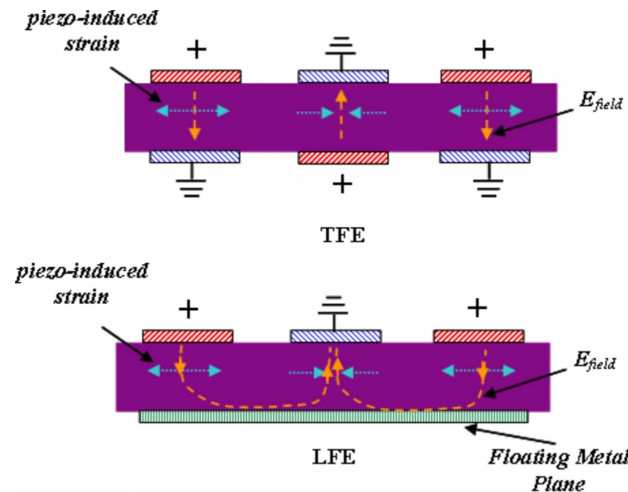

FIG. 2. (Color online) Two possible schemes of excitation of lateral modes of vibrations in AlN piezoelectric films. Electric field across the film thickness (which induces lateral strain in the piezoelectric film via the d_{31} coefficient) can be applied either via a TFE (top of figure) or a LFE (bottom of figure). The bottom floating electrode shown in the LFE embodiment is not necessary but helps to attain a better confinement of the electric field and a higher electromechanical coupling.

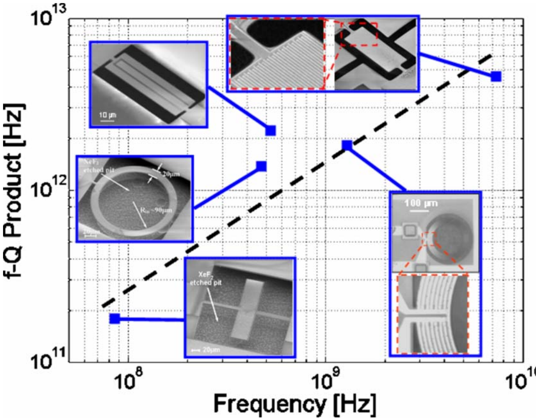

FIG. 3. (Color online) f-Q product vs frequency for some of the most significant AlN contour-mode devices. The highest f-Q product of 4.6×10^{12} has been recorded at 7.3 GHz (Ref. 34). These data show that unexpectedly, higher f-Q products than the one demonstrated at 20–1000 MHz can be achieved. This means that higher Qs should be attainable at lower frequencies. Further investigations into understanding the fundamental damping mechanisms of these devices are required.

B. MEMS AlN contour-mode oscillators

One of the largest application areas for resonators is timing. Although few electronic components have stood the test of time better than quartz crystal oscillators, MEMS-based solutions have emerged[12,13] as a very promising and competitive alternative due to its small form factor, high operating frequency, and especially the possibility to be fully integrated with integrated circuits (ICs). A key advantage of the AlN countor-mode technology over other MEMS implementations is its ability to offer impedances that can be directly interfaced with standard CMOS oscillator configurations such as Pierce, Colpitts, and Santos. Other unique features of the AlN technology are the capability of attaining multiple frequencies of operation on a single chip and withstanding large power. In fact the amplitude-frequency coefficient of an AlN resonator at 222 MHz was measured to be $\sim$8 ppm/mA^2, which is comparable to quartz crystal devices and about eight orders of magnitude better than electrostatic devices operating at few megahertz.[14] AlN contour-mode resonators at 176, 222, 307, and 482 MHz were connected to the same Pierce oscillator circuit (Fig. 4). These devices attained phase noise values between −88 and −68 dBc/Hz at 1 kHz offset frequency from the carriers and phase noise floors as low as −160 dBc/Hz at 1 MHz offset. The circuit was designed in the AMIS 0.5 μm 5 V CMOS process and consumes a static power of 10 mW. The characteristic phase noise response of a 222 MHz resonator is shown in Fig. 4. The phase noise of the 222 MHz oscillator operating at −4.8 dBm (Fig. 4) was also integrated from 12 kHz to 20 MHz and the rms jitter found to be 74 fS. This value is comparable to what is available from SAW-based oscillators working in the same frequency range.

As shown in Fig. 4, the current phase noise performances are limited by the circuit layout and further optimization is possible. In addition, by utilizing a more modern CMOS technology lower power consumption will also be possible.

C. MEMS AlN contour-mode filters

Another well established and probably even larger application area for resonators is filtering. Approximately 10–15 filters are present in most cell phones today and these numbers are steadily growing due to the need for multiple bands and applications. Filters are made out of array of resonators coupled either electrically or mechanically. The resonators are employed to precisely locate poles and zeros and achieve flat passband, sharp roll off, narrow bandwidth, and low loss filters.

Simpler to implement, electrical coupling requires routing of electrical signals from one device to the next without the need for any external electrical components. It is a robust coupling technique commonly used in MEMS and more generally for mechanical filters.[2,15–17] A very effective filter implementation using electrically cascaded AlN contour-mode resonators has been shown to work at 94 and 271 MHz (Ref. 17) (Table II). In this design, three or four two-port AlN resonators are connected in series and coupled by their intrinsic capacitance to realize high order filtering. This solution offers the possibility to design filters with good shape factors and off-band rejection without the need for different frequency devices as it is instead deemed necessary in ladder configurations.[2] This reduces the complexity of the filter design and fabrication and ultimately improves the device yield. Also, this coupling technique intrinsically provides for

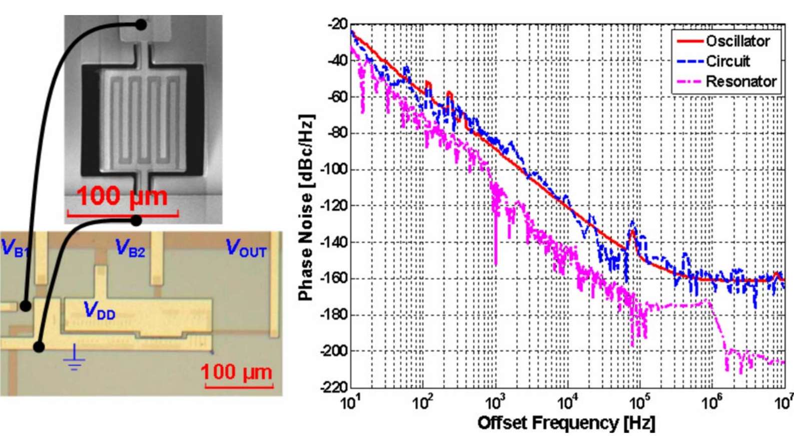

FIG. 4. (Color online) (Left) Picture of the demonstrated Pierce oscillator circuit (realized in the 0.5 μm 5 V AMIS process) and scanning electron micrograph of a 222 MHz AlN contour-mode resonators that was wirebonded to the circuit. (Right) Phase noise plot of the oscillator output. The continuous line overlaps with the dashed line, which represents the noise contribution from the circuit, whereas the dashed-dotted lines represent the noise contribution from the resonator. This preliminary data show that further improvement in oscillator phase noise can be attained by properly redesigning the circuit.

TABLE II. Summary of some characteristic results for AlN contour-mode resonant filters in the VHF range.

Filter Type	Scanning Electron Micrograph	Electrical Response (Transmission)	Key Features
Electrically Coupled [37] Cascaded Resonators)	Direct electrical couplers; Ground; Signal; Signal; Ground; 100 μm; Same frequency resonators	f_s = 271 MHz, IL= 4.2 dB, BW = 0.34 %, R_{term}= 2 kΩ; Magnitude of S21 [dB]; Frequency [MHz]	*- BW set by k_t^2 of device (0.1-1% possible)* *- Same frequency devices are needed (yield improvement)*
Hybrid Electrical and Mechanical Coupling [18]	Direct electrical coupler; 200 μm; 2nd order mechanical sub-filters	f_s = 110 MHz, IL= 5.2 dB, BW = 1.14 %, R_{term}= 800 Ω; Magnitude of S21 [dB]; Frequency [MHz]	*- BW is lithographically defined (1-2 % possible)* *- Smaller area for a given filter order*

[a]Reference 38.
[b]Reference 19.

narrow bandwidths (0.1%–0.4%), and makes the AlN technology a very good fit for the demonstration of channel-select filters (Table II). As will be highlighted in the next section, channel selection, instead of band selection represents a significant paradigm shift in the way current rf front ends are designed and can drastically reduce power consumption and architecture complexity.

Mechanical coupling requires the use of mechanical links between different resonators. Extensional beams[18] or solid quarter wave couplers (typical of monolithic filters) have been employed to realize these types of filter. It is generally difficult to realize high order filters simply by using mechanical elements because of excessive passband distortion and presence of spurious modes. Indeed, second order filters have shown to work reliably[19] and hybrid solutions that combine mechanical and electrical coupling to synthesize higher order filters are much more attractive. In fact hybrid coupling techniques leverage the advantages of mechanical coupling to demonstrated second order filtering functions in a small footprint with the ability of electrical coupling to provide effective out-of-band rejection and increased filter order. Table II shows such an implementation in which the AlN contour-mode devices take advantage of both electrical and mechanical coupling techniques to implement small form factor and high order filtering functions. The demonstrated 110 MHz filter shows a low insertion loss of 5.2 dB in air, a high out-of-band rejection greater than 65 dB, a fractional bandwidth as high as 1.14% (hard to achieve when only conventional electrical coupling is used), and unprecedented 30 and 50 dB shape factors of 1.93 and 2.36, respectively. All of these are achieved in an extremely small footprint and by using just half the space that any other fourth order filter would have taken. Each of the subfilters in Table II can be treated as a second order mechanically coupled filter stage for which the bandwidth is lithographically defined by the spacing between the input and output resonators. Electrical coupling (by simple cascading) of the two stages improves the out-of-band rejection of a single element and increases the filter order.

These results are important steps towards the demonstration of a technology capable of multifrequency filtering in the very high frequency (VHF) bands. Further explorations will lead to filters operating in the ultrahigh frequency bands, which are more largely employed in most modern rf systems.

III. MEMS ALN SWITCH TECHNOLOGY

In order to impact size, power consumption, and spectral efficiency of current rf front ends and enable next generation architecture based on massive arraying of AlN micromechanical resonant devices, an AlN MEMS switch that can be monolithically integrated with the resonator technology has been developed.[20] An integrated solution greatly reduces the parasitic elements introduced by bonding of different technologies and the overall size of the rf analog module.

Although significant progress has been made in the demonstration of rf MEMS switches, just few research groups have looked at piezoelectric actuation.[21–24] Electrostatic,[25–27] electromagnetic,[28,29] and thermoelastic[30] actuation have been primarily used in rf MEMS switches. Electromagnetic and thermoelastic actuation methods require high power consumption for actuation (few milliwatts per device) and are incompatible with modern low power rf front ends. Electrostatic actuation is the most commonly used actuation method. Although easily integrated, from a fabrication process perspective, with other technologies (such as the AlN

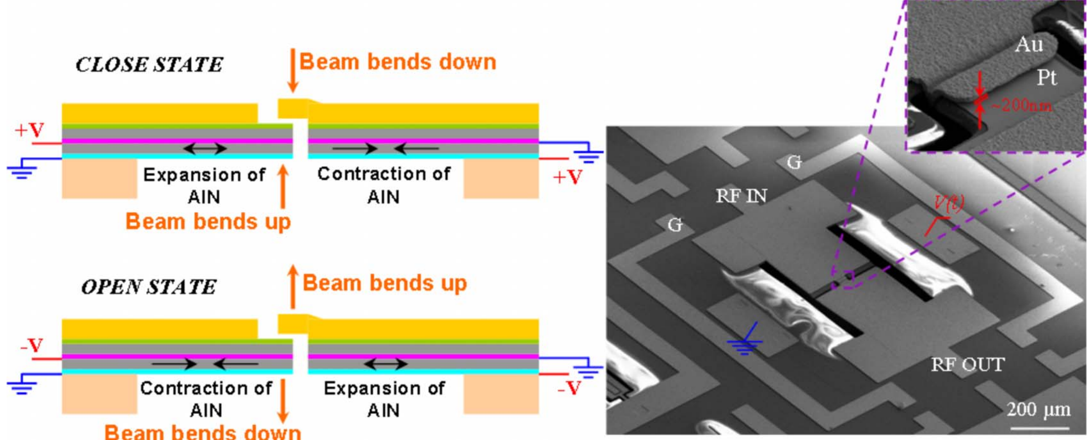

FIG. 5. (Color online) (Left) Schematic representation of the principle of operation of a dual-beam AlN MEMS switch. (Right) Scanning electron micrograph of the dual-beam AlN MEMS switch. The inset shows a detail of the Au–Pt contact and the nanogap formed by a thin a-Si sacrificial layer.

resonator), this actuation mechanism requires high voltages (>50 V) that necessitate the presence of a separate on-chip high voltage source or charge pump to operate the switch. Furthermore, electrostatic actuation does not provide for active pull-off forces to release the switch after contact and relies exclusively on the device spring constant. This is an important factor to be considered in the choice of the actuation mechanism since most contact switches demonstrated to date tend to fail stuck close. AlN piezoelectric actuation can instead overcome most of these drawbacks and can also be directly integrated with the AlN contour-mode resonator technology.

As shown in Fig. 5, the demonstrated AlN MEMS switch is composed of two opposed bimorph beams formed by a stack of AlN, platinum (Pt) and gold. The Pt electrodes are used to establish an electric field across the piezoelectric layer, whereas the electroplated gold layer fulfills the double purpose of offsetting the neutral axis of the piezoelectric beam (to induce bending in the bimorph) and carrying the rf signal. The innovative design based on the use of two opposing beams is advantageous from a fabrication as well as performance perspective. The use of two movable elements to define the isolation gap between the contacts greatly relaxes the manufacturing tolerances to stresses, which are hard to eliminate by simply acting on thin film deposition techniques. In addition, the use of two beams doubles the contact forces and reduces the switching time for a given actuation voltage, since each of the beams needs to travel half of the total size of the gap.

The fabricated AlN switches were tested for dc and rf performances. dc resistance (R_{on}) measurements of the switches show that the contact resistance decreases with the applied voltage, proving that higher forces produce lower contact resistance. As previously described, the dual-beam actuation scheme takes advantage of this concept and uses two actuators to double the force per unit applied voltage. The existing contacting metals are Au and Pt and R_{on} in the range of $2-3\ \Omega$ have been attained in switches with large contact area ($10\times 10\ \mu m^2$) for voltages varying between 20 and 40 V. The R_{on} of the switch can be further reduced if different contact materials with low resistivity, such as rhenium and gold palladium alloys are used. In addition to the contact material, roughness of the contact surface and contamination around the contact area are considered to be other mechanisms, which can strongly affect the contact resistance of the switch. These mechanisms can be mitigated by using other deposition techniques for the sacrificial layer (done by evaporation in this implementation) or by improving the cleanliness of the contact area by means of packaging, nitrogen flowing or heating of the switch to remove any organic layer in the contact area.

Preliminary rf measurements were performed in order to verify the rf response of this first AlN switch prototype. Figure 6 presents the isolation and the insertion loss of a dual-beam AlN switch. In this switch, isolation >26 dB and low return loss (RL) <0.75 dB at 2 GHz were obtained. The current isolation response is limited by a combination of the switch contact size, gap dimensions, and parasitics. The off-state capacitance is in fact 42 fF at 2 GHz and it is about eight times the design value. Insertion loss (IL) <0.67 dB and RL >34 dB were recorded at 2 GHz for this same switch. The higher than expected IL value is likely due to

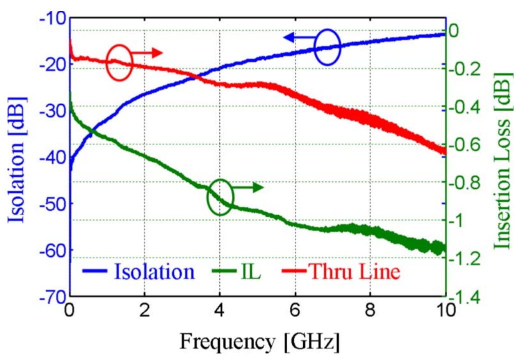

FIG. 6. (Color online) Measurement of isolation and IL for a dual-beam AlN switch from 10 MHz to 10 GHz. Switch IL is compared to the loss in a through line of comparable length.

substrate parasitics and an unwanted coupling between rf and dc signals, which can be warranted by improved care in the layout of the actuation signal.

IV. MEMS INTEGRATED RF FRONT ENDS

Novel rf architectures that take advantage of high Q microelectromechanical resonant devices have already been proposed by circuit designers[31,32] and rf MEMS experts.[33] The ability to array multiple filtering components on the same chip is particularly attractive for the deployment of next generation software defined cognitive radios, which will require spectrum-aware components capable of rapid reconfiguration and high rejection of interferers. In order to reduce power consumption in analog to digital converters (ADC), channel select instead of band-select filters, will need to be implemented. The fundamental bottlenecks to such realization reside in the absence of switched filter banks simultaneously capable of high Q, small impedances, and monolithic integration with switches. The AlN contour-mode technology embodies the first two characteristics, but has so far lacked the ability to be switched on and off. The following sections highlight the key steps that brought to the demonstration of the first monolithic integration of the aforementioned MEMS AlN contour-mode resonator and switch technologies. Initial device performance is then analyzed and new rf front-end architectures enabled by this new platform are presented.

A. Fabrication process and integrated device performance

A major hurdle to overcome for the demonstration of switched filter banks was the physical integration of two dissimilar technologies such as the MEMS AlN resonator and switch. Although the same transduction mechanism is used, the two devices have different material and fabrication requirements that needed to be taken into account. The AlN resonator technology is further along in its development and metal to resonator thickness ratio have already been optimized. This constrained the design space for the AlN switch technology, for which the electroplated gold layer was introduced to compensate for limitation in the design thicknesses available from the AlN film. In addition, the materials for forming a sacrificial gap and the electroplating step had to be selected in order to be compatible with the underlying components. For this reason a low-temperature amorphous silicon layer was used and a seed layer such as NiCr, whose etchant is compatible with AlN, was employed during the electroplating step. The first integration resulted in a seven mask fabrication process which is capable of simultaneously yielding high performance resonators and switches. The fabrication process consists of rather conventional IC manufacturing steps and is briefly presented in Fig. 7.

Although in this first implementation the AlN resonator and switch were not directly connected (as shown in Fig. 8), it was still possible to separately probe resonators and switches cofabricated on the same die. In order to prove that effective integration of the two technologies can ultimately

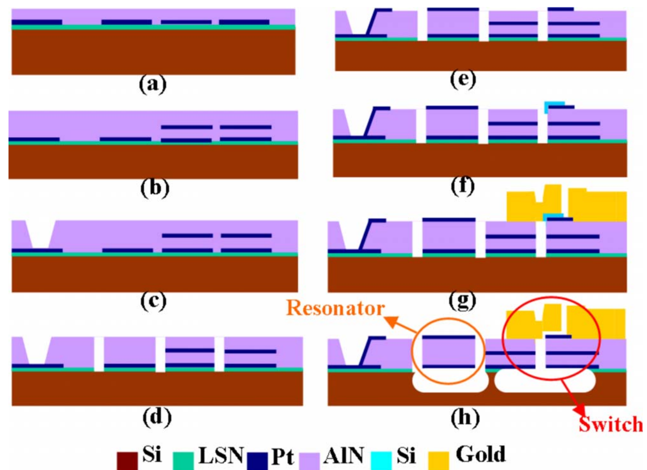

FIG. 7. (Color online) Process flow used for the monolithic integration of the dual-beam switch with contour-mode resonators. (a) First AlN layer deposition by sputtering on top of Pt and LSN. (b) Second AlN layer sputtering on top of an intermediate Pt layer. (c) Opening of via to bottom and middle Pt. (d) AlN etch using Cl_2-based reactive ion etching. (e) Top Pt deposition and patterning by lift-off. (f) Evaporation of amorphous Si sacrificial layer and patterning by lift-off. (g) Gold electroplating. (h) XeF_2 release of structures. The dry release removes both the sacrificial layer and the underlying substrate without any stiction issues

provide for switched filter banks and frequency setting elements, the response of a 224 MHz resonator was cascaded to the one of a switch fabricated in the same process. The cumulative response (Fig. 9) shows that the introduction of the switch does not alter the resonator core parameters (Q =2000 and k_t^2=2%) and effectively turns the resonator off when in the open state. The cascaded performance in the off state can be further improved at higher frequencies, at which lower substrate parasitics have been recorded.

B. Novel integrated rf front ends

The multifrequency and reconfigurable monolithic technology platform (resonator, filters and switches) that is under development can be applied to different communication systems and represents a paradigm shift in the way rf signal processing is performed. By taking advantage of the possibility to array banks of switched narrow-band filters at different frequencies, previously envisioned, but never implemented, rf front ends can be made possible. For example, channel selection in wideband code-division multiple-access can be implemented by arraying twelve distinct filters with a fractional bandwidth of approximately 0.25% (12 5 MHz channels spaced 200 kHz apart around 2 GHz). The filter bank can be employed to directly select the carrier signal before downconversion in low-intermediate frequency (IF) or direct conversion receivers (Fig. 1). The proposed architecture significantly reduces the power consumption in low noise amplifiers, mixers, and voltage controlled oscillators by improving rejection directly at the channel and relaxing the linearity requirements on the electronic components and the phase noise of the oscillator.

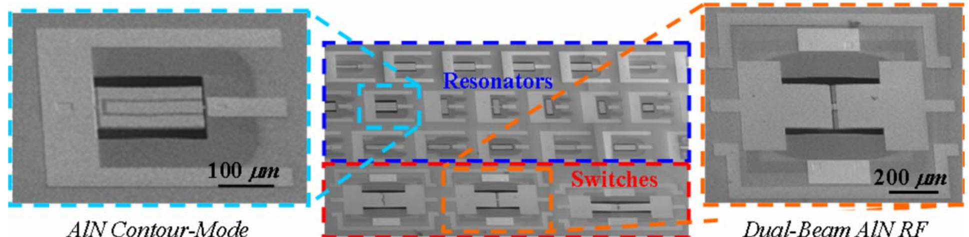

FIG. 8. (Color online) Scanning electron micrograph showing the physical integration of AlN contour-mode resonators with dual-beam AlN rf switches. Although no interconnects were present in this first implementation, individual devices representative of both technologies had been fabricated and tested on the same die and their combined responses are shown in Fig. 9.

Future software defined radios will also have similar requirements in terms of front-end filtering. In order to reduce power consumption in the ADC, direct channel sampling at the antenna location needs to be implemented by means of switched arrays of narrow-band filters (Fig. 1). In this case, a very large area of the available spectrum (300 MHz–5 GHz, for example) needs to be covered: Large scale integration of microelectromechanical devices will make this possible.

V. CONCLUSIONS

The latest research efforts underway at the University of Pennsylvania for the development of monolithically integrated MEMS AlN rf front ends have been presented. Experimental results on AlN contour-mode resonators and switches have been shown to demonstrate the ability of this technology to deliver small form factor and low power frequency reference elements, filtering components, and switching devices. A monolithically integrated solution that directly combines the resonator and switch technologies has been presented and the key material and fabrication challenges that had to be overcome for its implementation have been discussed. Novel rf architectures that take advantage of large scale integration of AlN MEMS devices have been introduced as revolutionary designs that will significantly reduce power consumption in modern communication systems and will enable next generation software defined radios. Despite the noteworthy progress that has been made with the AlN MEMS technology, there are still significant challenges that need to be addressed in terms of characterizing these devices to meet specifications for power handling, temperature stability, and packaging as well as improving the resonator quality factor and electromechanical coupling and the switch insertion loss and reliability. These topics are the subject of ongoing research.

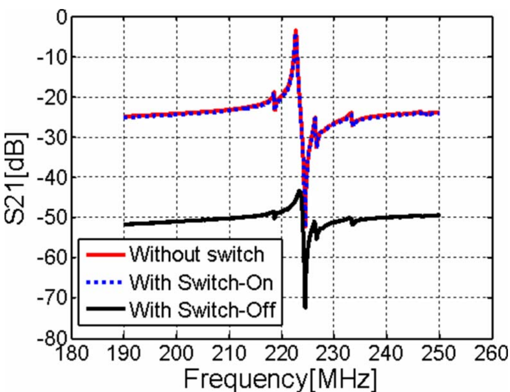

FIG. 9. (Color online) S_{21} plot (cascaded S parameters) of a contour-mode resonator monolithically integrated with the AlN switch. The response of a resonator with the switch in both on and off states is shown. No significant changes in the resonator response were recorded, to the point that the resonator response without the switch is completely overlapped by the curve with the switch in the on position. The resonator is effectively turned off by the switch.

ACKNOWLEDGMENTS

The author would like to thank his graduate students Chengjie Zuo, Nipun Sinha, Matteo Rinaldi, and Chiara Zuniga and postdoctorates Rashed Mahameed and Marcelo Pisano for their efforts in the development of the presented work. Many thanks also to Justin Black and Phil Stephanou at Harmonic Devices, Inc. for providing some of the experimental results and actively seeking the commercialization of the AlN technology.

[1]R. Ruby and P. Merchant, *IEEE International Frequency Control Symposium* (IEEE, New York, 1994), pp. 135–138.
[2]R. Ruby, P. Bradley, J. Larson, III, Y. Oshmyansky, and D. Figueredo, *IEEE International Solid-State Circuits Conference* (IEEE, New York, 2001), pp. 120–121.
[3]W. Jing, J. E. Butler, T. Feygelson, and C. T. C. Nguyen, *MEMS 2004, 17th IEEE International Conference on Micro Electro Mechanical Systems* (IEEE, New York, 2004), pp. 641–644.
[4]S. Pourkamali, H. Zhili, and F. Ayazi, J. Microelectromech. Syst. **13**, 1054 (2004).
[5]L. Yu-Wei, L. Sheng-Shian, X. Yuan, R. Zeying, and C. T. C. Nguyen, *Frequency Control Symposium and Exposition, 2005* (IEEE, New York, 2005), pp. 128–134.
[6]M. Aissi, E. Tournier, M. A. Dubois, C. Billard, H. Ziad, and R. Plana, *IEEE Radio Frequency Integrated Circuits (RFIC) Symposium* (IEEE, New York, 2006), p. 4.
[7]M.-A. Dubois, C. Billard, J.-F. Carpentier, P. Vincent, G. Parat, and C. Muller, *IEEE Ultrasonics Symposium* (IEEE, New York, 2005), pp. 85–88.
[8]B. Antkowiak, J. P. Gorman, M. Varghese, D. J. D. Carter, and A. E. Duwel, *TRANSDUCERS '03, 12th International Conference on Solid-State Sensors, Actuators and Microsystems*, 2003 (unpublished), pp. 841–846.
[9]D. J. D. Carter, D. J. Kang, D. White, and A. Duwel, *Hilton Head Workshop 2008, Solid-State Sensors, Actuators and Microsystems Workshop* (Transducer Research Foundation, 2004), pp. 841–846.
[10]G. Piazza, P. J. Stephanou, and A. P. Pisano, Solid-State Electron. **51**, 1596 (2007).
[11]A. Ballato and J. G. Gualtieri, IEEE Trans. Ultrason. Ferroelectr. Freq.

Control **41**, 834 (1994).
[12]L. Yu-Wei, L. Seungbae, L. Sheng-Shian, X. Yuan, R. Zeying, and C.-C. Nguyen, *IEEE International Solid-State Circuits Conference* (IEEE, New York, 2004), Vol. 1, pp. 322–530.
[13]G. K. Ho, K. Sundaresan, S. Pourkamali, and F. Ayazi, *18th IEEE International Conference on Micro Electro Mechanical Systems* (IEEE, New York, 2005), pp. 116–120.
[14]M. Agarwal*et al.*, *Solid State Sensor, Actuator and Microsystems Workshop (Hilton Head 2006)* (IEEE, New York, 2006).
[15]G. Piazza, P. J. Stephanou, and A. P. Pisano, J. Microelectromech. Syst. **16**, 319 (2007).
[16]S. V. Krishnaswamy, J. Rosenbaum, S. Horwitz, C. Vale, and R. A. Moore, *IEEE 1990 Ultrasonics Symposium* (IEEE, New York, 1990), pp. 529–536.
[17]Z. Chengjie, N. Sinha, M. B. Pisani, C. R. Perez, R. Mahameed, and G. Piazza, *IEEE Ultrasonics Symposium, 2007* (IEEE, New York, 2007), pp. 1156–1159.
[18]P. J. Stephanou, G. Piazza, C. D. White, M. B. J. Wijesundara, and A. P. Pisano, J. Phys.: Conf. Ser. **34**, 342 (2006).
[19]C. Zuo, N. Sinha, C. R. Perez, R. Mahameed, M. B. Pisani, and G. Piazza, *Solid State Sensor, Actuator and Microsystems Workshop (Hilton Head 2008), South Carolina, USA* (Transducer Research Foundation, 2008).
[20]R. Mahameed, N. Sinha, M. B. Pisani, and G. Piazza, J. Micromech. Microeng. **18**, 11 (2008).
[21]H. C. Lee, J. H. Park, J. Y. Park, H. J. Nam, and J. U. Bu, J. Micromech. Microeng. **15**, 2098 (2005).
[22]J. H. Park, H. C. Lee, Y. H. Park, Y. D. Kim, C. H. Ji, J. Bu, and H. J. Nam, J. Micromech. Microeng. **16**, 2281 (2006).
[23]S. J. Gross, S. Tadigadapa, T. N. Jackson, S. Trolier-McKinstry, and Q. Q. Zhang, Appl. Phys. Lett. **83**, 174 (2003).
[24]B. Piekarski, M. Dubey, E. Zakar, R. Polcawich, D. DeVoe, and D. Wickenden, Integr. Ferroelectr. **42**, 25 (2002).
[25]P. M. Zavracky, S. Majumder, and N. E. McGruer, J. Micromech. Microeng. **6**, 3 (1997).
[26]S. Pranonsatit, A. S. Holmes, I. D. Robertson, and S. Lucyszyn, J. Micromech. Microeng. **15**, 1735 (2006).
[27]G. M. Rebeiz and J. B. Muldavin, IEEE Microw. Mag. **2**, 59 (2001).
[28]Y. H. Zhang, G. F. Ding, X. F. Shun, D. H. Gu, B. C. Cai, and Z. S. Lai, Sens. Actuators, A **134**, 532 (2007).
[29]D. Hyman*et al.*, Int. J. RF Microwave Comput.-Aided Eng. **9**, 348 (1999).
[30]R. D. Streeter, C. A. Hall, R. Wood, and R. Madadevan, Int. J. RF Microwave Comput.-Aided Eng. **11**, 261 (2001).
[31]S. Kiaei, S. M. Taleie, and B. Bakkaloglu, *IEEE International Symposium on Circuits and Systems (ISCAS)* (IEEE, New York, 2005), pp. 4401–4405.
[32]S. M. Taleie, Z. Jiandong, and S. Kiaei, *The 2004 47th Midwest Symposium on Circuits and Systems* (IEEE, New York, 2004), pp. 363–366.
[33]C. T. C. Nguyen, IEEE Trans. Ultrason. Ferroelectr. Freq. Control **54**, 251 (2007).
[34]M. Rinaldi, C. Zuniga, and G. Piazza, to be presented at the 22nd IEEE International Conference on MicroElectroMechanical Systems, 2009 (unpublished).
[35]G. Piazza, P. J. Stephanou, and A. P. Pisano, J. Microelectromech. Syst. **15**, 1406 (2006).
[36]P. J. Stephanou and A. P. Pisano, *IEEE Ultrasonics Symposium* (IEEE, New York, 2006), p. 4.
[37]P. J. Stephanou and A. P. Pisano, *20th IEEE International Conference on Micro Electro Mechanical Systems-MEMS* (IEEE, New York, 2007), pp. 787–790.
[38]C. Zuo, N. Sinha, M. B. Pisani, C. R. Perez, R. Mahameed, and G. Piazza, *Ultrasonics Symposium, 2007* (IEEE, New York, 2007), pp. 1156–1159.